

First Principles Study of Electronic Structure of Transition Metal Nitride: TiN under Normal and High Pressure

A.T. Asvini Meenaatci¹, *R. Rajeswarapalanichmy¹
and K. Iyakutti²

¹*Department of Physics, N.M.S.S.V.N. College,
Madurai, Tamilnadu, India.*

²*School of Physics, Madurai Kamaraj University, Tamilnadu, India.*

**Corresponding Author E-mail: rrpcaspd2003@yahoo.com*

Abstract

First principles calculation were performed using Tight-binding LMTO method with Local density approximation (LDA) and Atomic sphere approximation (ASA) to understand the electronic properties of Titanium nitride. The equilibrium geometries, the electronic band structure, the total and partial DOS are obtained under various pressures and are analyzed in comparison with the available experimental data. The most stable structure of TiN is NaCl like structure. Our results indicate that TiN can be used as a hydrogen storage material. We estimated the average electron-Phonon coupling constant to be 0.59 and superconducting Transition Temperature (T_c) is 6.089K. The T_c value increases with increase in pressure.

Keywords: Titanium nitride; Electronic structure; structural phase transition; Superconducting transition temperature.

Pacs No.: 31.15.A-,74.25.-q, 61.50.Ks.

Introduction

Transition metal nitrides are of intense interest for researchers because they have important technical applications such as oxidation resisting material [1] and in optical and magnetic apparatus [2]. Transition metal nitrides posse's particular mechanical, optical, electronic and magnetic properties [3], which are attributed to their unusual electronic bonding (a mixture of covalent, ionic bonding) and strong electron phonon

interaction. Liping ZHU, Masao ohanshi and Shoji Yamanaka reported the superconducting property by chemical synthesis method [4]. TiN with face centered cubic structure was observed and the corresponding T_c value, 4.5-6.0K, was obtained. Dong CHEN Jingdong CHEN, Yinglu ZHAO, Benhai YU, Chunlei WANG and Deheng SHI [5] estimated the elastic properties of TiN by (PW-PP) method. But they have not investigated the effect of pressure on the band structure, density of states and super conducting transition temperature. Moreover, to the best of our knowledge, the structural phase transition and charge density distribution of TiN has also been not reported yet.

In this paper, the band structure, density of states (DOS), electronic Charge distribution, structural phase transition and superconductivity of TiN under various pressures are investigated by first principles calculation. Most of transition metal mononitrides are known to be generally based on cubic or hexagonal metal sub lattice and N atoms occupy octahedral or trigonal prismatic interstitial sites. Hence, all the possible cubic and hexagonal are chosen as candidate structure of TiN, including Zinc blende (ZB) (space group $F\bar{4}3m$), rock salt (NaCl) (space group $Fm\bar{3}m$), and WC (space group $P\bar{6}m2$). Further, the superconducting transition temperature T_c of TiN is estimated by using McMillan Formula [6].

Computational details

The calculations presented in this paper was carried out using tight binding linear muffin tin orbital method. This method treats the one electron potential in relativistic form. In the LMTO scheme the crystal potential is approximated by a series of non-overlapping atomic like potential and a constant potential (muffin tin potential) among spheres. The Schrodinger equation can be solved in both regions. These solutions are then matched at the sphere boundaries to produce muffin tin orbital. This muffin tin orbital's are used to construct a basis which is linear order in energy and rapidly convergent [7-10]. Pressure calculations are done with second order Birch Murnaghan equation of states [11-12]. The Young's modulus and Poisson ratio are calculated by the formula $E = 9BG/(3B+G)$, $\nu = 3B-2G/2(3B+G)$.

Result and discussions

Mechanical property

Equilibrium volume $V_0(\text{\AA}^3)$, lattice parameters $a(\text{\AA}^3)$, $c(\text{\AA}^3)$, Valence electron density ρ (electrons/ \AA^3), bulk modulus B_0 and its derivative B_0' , total energy (Ry), Density of states (DOS) at the Fermi level $N(E_F)$ (Dos(States/Ry.Cell)), Radius of the Wigner-Seitz cell (R_{wz}), Young's modulus E (GPa), shear modulus G (GPa), Poisson ratio ν obtained from TB-LMTO method are given in table.1. The three independent elastic constants C_{ij} (C_{11} , C_{12} , C_{44}) should satisfy the well known Born-Huang criteria for the stability of cubic crystals [13].

$$C_{44} > 0, C_{11} > |C_{12}|, C_{11} + 2C_{12} > 0$$

Table 1: Equilibrium volume $V_0(\text{\AA}^3)$, lattice parameters $a(\text{\AA}^3), c(\text{\AA}^3)$, Valence electron density ρ (electrons/ \AA^3), bulk modulus B_0 and its derivative B_0' , total energy (Ry), Density of states (DOS) at the Fermi level $N(E_f)$ (Dos(States/Ry.Cell)), Radius of the Wigner-Seitz cell (Rwz), Young's modulus $E(\text{GPa})$, shear modulus $G(\text{GPa})$, Poisson ratio ν .

	ZB-TiN	NaCl-TiN	WC-TiN
V_0	19.0562	23.7043	19.4162
a	4.5468	4.2743	2.7476
c			2.978
ρ	0.4722	0.3796	0.4635
B_0	264	339	112
B_0'	3.9	4.729	4.319
$N_f(E_f)$	19.2515	27.7603	21.5657
ν		0.13	
E	115	239	152
G	165	229	53
Rwz	2.3289	1.9891	2.1875
$E(\text{total})$	-1813.6485	-1814.0489	-1813.9332

Clearly, the obtained elastic constants of cubic NaCl-TiN satisfy that the Born-Huang criteria, suggesting that it is mechanically stable. The elastic constants obtained using TB-LMTO method are compared with the available experimental [14] and theoretical data [5][15-18] in table.2. From the table.2, it is found that our result agrees with the experimental as well as the theoretical work. The equilibrium volumes per f.u are 23.7002\AA^3 for ZB-TiN, 19.0562\AA^3 for NaCl-TiN, 19.4163\AA^3 for WC-TiN, which are higher than that of Ti metal (14.6743\AA^3) due to the addition of N atoms. Valence electron density (VED) is the total number of valence electrons divided by volume per unit cell which is an important factor for analyzing the super hard materials. The calculated VEDs are $0.3797 \text{ electrons}/\text{\AA}^3$ for ZB-TiN, $0.47226 \text{ electrons}/\text{\AA}^3$ for NaCl-TiN and $0.4635 \text{ electrons}/\text{\AA}^3$ for WC-TiN. It is worth noting that all VEDs for these structures are higher than that of Ti metal ($0.3261 \text{ electrons}/\text{\AA}^3$) [19] and are comparable to $0.70 \text{ electrons}/\text{\AA}^3$ for diamond [20]. Young's modulus E and Poisson's ratio are the two important factors for technological and engineering application. The stiffness of the solid can be analyzed using the young's modulus (E) value. From the table.1, it is clear that the bulk modulus of TiN is larger than that (339 GPa) of Ti metal except for WC-TiN (unstable mechanically). Thus, we conclude that the TiN is less compressible than the pure Ti. Poisson ratio reflects the stability of the crystal against shear.. The ratio can formally take values between -1 and 0.5, which corresponds to the lower limit where the material does not change its shape or to the upper limit when the volume remains unchanged. The obtained Poisson ratio of NaCl-TiN is 0.13 which indicates that TiN has central interatomic forces and is relatively against shear. The high G/B ratio also implies a high degree of covalency. To discuss the incompressibility of TiN, the evolution of volume

compression as a function of pressure is plotted in fig.1. For comparison the volume compression of diamond is given as well. It is evident that NaCl-TiN has almost the same incompressibility as diamond between 0 and 34.97GPa and the incompressibility is even higher than that of diamond in the 80-700GPa range, Which can be explained by the strong electronic repulsion and the strong covalence bonding between Ti and N atoms. The case that the incompressibility exceeds that of diamond was also found in ReC[21].

Table 2: Comparison of elastic constants of stable NaCl-TiN with previous experimental and theoretical work at normal pressure.

Bo (GPa)	Bo'	C ₁₁ (GPa)	C ₁₂ (GPa)	C ₄₄ (GPa)
339	4.2	635	187	225
318 ¹⁴	4.0 ¹⁴	625 ¹⁴	165 ¹⁴	168 ¹⁴
286 ¹⁵		610 ⁵	100 ⁵	169 ⁵
304 ¹⁶				
326 ¹⁷				
318 ¹⁸				

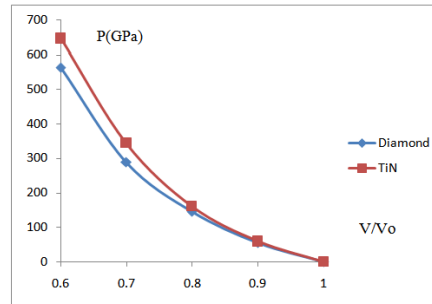


Figure 1: Volume as a function of pressure with respect to the equilibrium volume, V_0 .

Electronic structure

The band structure of TiN is computed for various pressures and the band structure for normal and high pressure is given in fig.2. From the figure.2, it is seen that, at normal pressure, the band structure of TiN has 4 valence bands (Bottom most) corresponding to 9 valence electrons which comes from $3d^2 4s^2$ of Ti atom and $2s^2 2p^3$ state electrons of N atom. Above the Fermi level the empty conduction bands are present with a mixed s, p, d characters. The empty conduction bands are highly overlapping with the valence bands and there is no band gap. Hence, at normal pressure TiN is metallic. Electrons in s, p and d shells of Ti and N at different pressures for NaCl-TiN are given in table.3. From the table.3, it is found that as the pressure increases, a fraction of 4s and 3d state electrons are transferred to the 4p state

of Ti atom. Similarly, a portion of 2s electrons are transferred to 2p and 3d states of N atom. At high pressure the bands get dispersed. To understand the correlation between the electronic and mechanical properties, we have computed the density of states under equilibrium geometry. The total and partial DOS of TiN are shown in fig.3. The obtained DOS at the Fermi level $N_I(E_F)$ are given in table.1. From the fig.3, it is observed that the electrons from Ti-3d and the N-2p state contribute much to the DOS near the Fermi level. The peak emerging in the lower-energy region of the DOS curve mainly originates from the localized s-state of N atom. The energy region just above the Fermi level is dominated by unoccupied Ti-d states. In the DOS of NaCl-TiN, the highest spike is due to 3d state electrons of Ti atom. As the pressure increases, the height of the spike decreases. A pseudo gap is observed in this histogram. The DOS of Ti-d and N-p states are energetically degenerate from the bottom of the valence band to the top of the conduction band, indicating the possibility of covalent bonding between Ti and N atom. The covalent characteristics between Ti and N atoms can be confirmed by the charge density distribution. The charge density distribution for NaCl-TiN is shown in Fig.4. It is clearly seen that charge strongly accumulates between Ti and N atoms, which means that a strong directional bonding exists between them. The total charge transfer from Ti to N in NaCl-TiN implies that the chemical bonding between Ti and N atoms have some ionic character. Thus, our results demonstrate that the bonding should be a mixture of metallic, covalent and ionic attribution in TiN.

Table 3: Electrons in s, p and d shells of Ti and N at different pressures for NaCl-TiN.

P (GPa)	Ti			N		
	4s2	4p0	3d2	2s2	2p3	3d0
Normal	0.3097	0.5801	2.2863	1.5872	3.5922	0.0720
59.576	0.2968	0.5927	2.2762	1.5539	3.5837	0.0809
161.8580	0.2830	0.7042	2.1928	1.5160	3.5667	0.0886
344.6935	0.2927	0.5977	2.2713	1.5434	3.5841	0.0839
646.8121	1.9369	3.3933	0.2002	1.4846	1.6067	0.0675

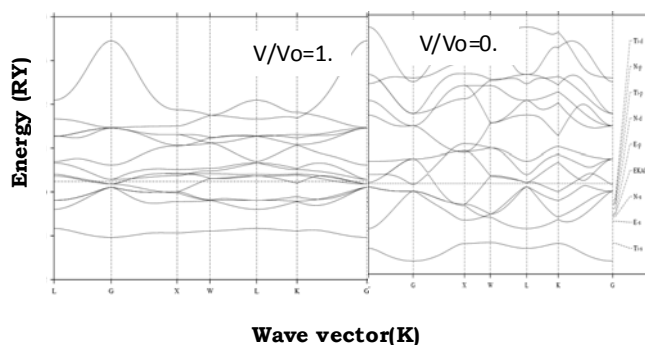


Figure 2: Band structure of NaCl-TiN at Normal pressure and high pressure.

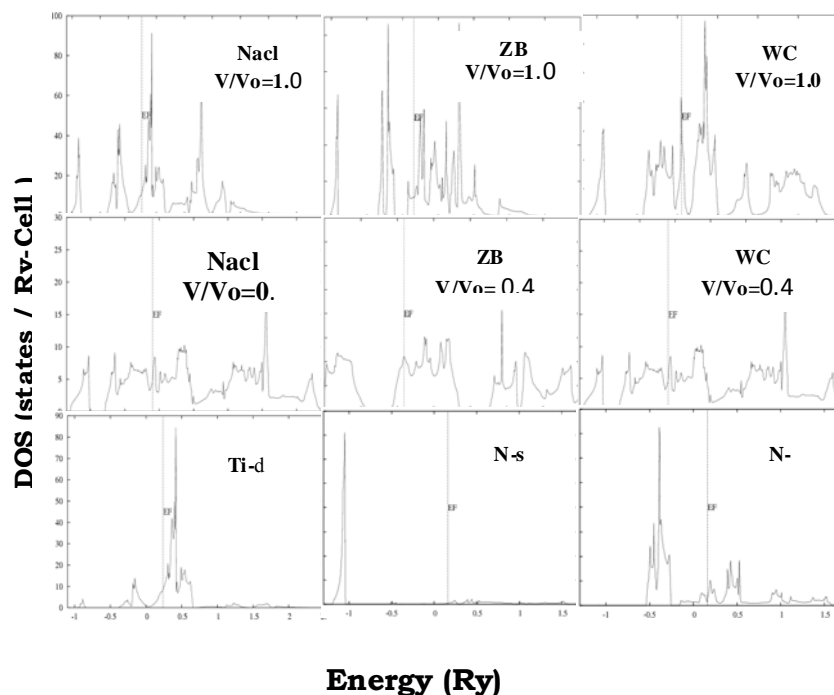


Figure 3: Total DOS of TiN for different phases and partial DOS at Normal and high pressure.

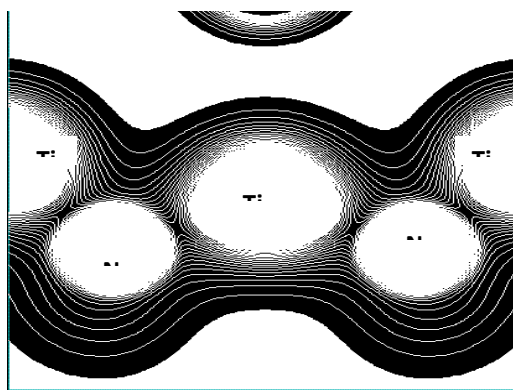


Figure 4: Charge density plot of NaCl-TiN at Normal pressure.

Energetics and phase diagram

The energy- V/V_0 curves corresponding to the three different phases of TiN are shown in fig.5, where V/V_0 is the ratio between volumes at any pressure to the equilibrium volume. At normal pressure, the thermodynamically stable phase of TiN is NaCl structure. It is observed that a structural phase transition from cubic ZB phase to cubic NaCl phase at 34.97 GPa. Hence, at high pressure TiN is stable with cubic NaCl phase.

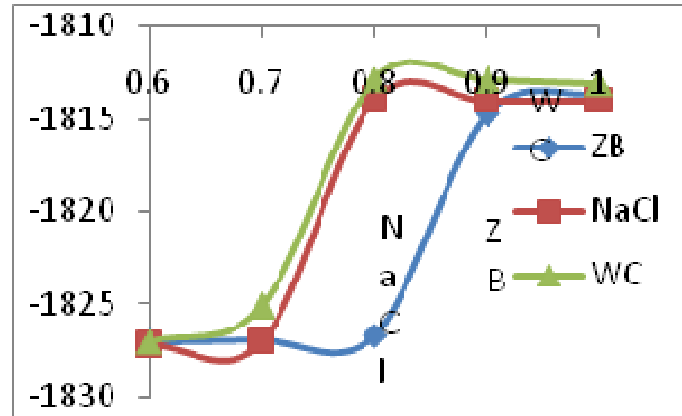


Figure 5: Structural Phase transition between Hexagonal Wc TiN and cubic-NaCl,ZB TiN phases.

Superconducting Transition Temperature (T_c K)

The Debye temperature of NaCl-TiN is 600K, which indicates that TiN may be superconductor. So we further estimate the superconducting transition temperature of TiN with McMillan equation [6]. λ , μ^* and T_c values as a function of pressure for TiN with constant Debye temperature [$\theta_D=600$ K] are given in table.4. At normal pressure, the calculated electron-phonon coupling constant λ is 0.59 and the estimated superconducting Transition Temperature (T_c) is 6.089K [22-23] for the screened coulomb potential (μ^*) 0.1697. The T_c value increases with increase in pressure. The variation of T_c with pressure is shown in fig.6. The computed superconducting transition temperature for the normal pressure is compared with the available experimental [4][14] and other theoretical work [5] in table.5. From the table.5, it is found that our result is in agreement with the experimental as well as the theoretical work.

Table 4: λ , μ^* and T_c values as a function of pressure for TiN with constant Debye temperature [$\theta_D=600$ K].

P (GPa)	λ	μ^*	T_c (K)
Normal	0.59	0.145	6.089
59.576	0.632	0.149	7.6014
161.8580	0.748	0.151	13.1399
344.6935	0.875	0.156	191336

Table 5: Comparison of superconducting Transition Temperature (Tc K) and elastic constants with previous experimental and theoretical work at normal pressure.

Pressure (Gpa)	λ	μ^*	Tc (K)
Normal pressure	0.59	0.145	6.089
	0.59 ²³	0.145 ²²	6.0 ²²
	0.541 ²⁴	0.13 ²⁴	6.02 ²³
			5.49 ²⁴

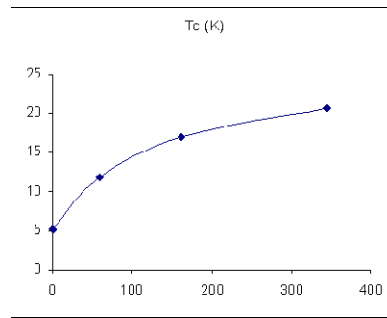


Fig.6: Tc (K) Vs Pressure (GPa) curve

Hydrogen storage in TiN

Hydrogen fuel, which can be readily produced from renewable energy sources, contains at least three times larger chemical energy per mass $\sim 142 \text{ MJ kg}^{-1}$ than any chemical fuel, thus making a hydrogen fuel cell an attractive alternative to an internal combustion engine for transportation. Elements, especially those in groups I–IV and some transition metals, have their nitride, hydride and amide/imide forms. There is, therefore, still plenty of scope for further exploring metal–N–H systems for hydrogen storage. In our study, we doped a hydrogen molecule with TiN. The band structure of H_2 doped TiN at Normal pressure is given in fig.7. From the figure it was observed that the bands due to H-s state lies near the Fermi level. The total energy of TiNH_2 was -1815.990 Ry , which is smaller than that of TiN. Therefore, at normal pressure TiNH_2 is stable. Thus, our results demonstrate that TiNH_2 can be used as a hydrogen storage material.

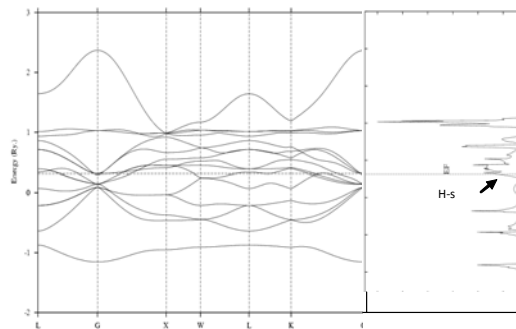


Figure 7: Band structure of H_2 doped TiN at Normal pressure.

Conclusion

The band structure, density of states, structural phase transition, charge density and superconducting transition temperature under various pressures are investigated based on first-principles calculation under the frame work of tight-binding theory within local density approximation. At normal pressure, the thermodynamically stable phase has NaCl structure. High valence electron density and bulk modulus indicate that TiN is a super hard conductor. Electronic structure calculations show that TiN presents obvious metallic features. In particular, the calculated superconducting Transition Temperature (about 6.089K) for cubic NaCl-TiN agrees well with the experimental value. The superconducting Transition Temperature (T_c K) increases with increase in pressure. Strong hybridization between metal d electrons and nonmetal p electrons indicate that there is a strong covalent bonding between Ti and N atoms. Our results indicate that TiN can be used as a hydrogen storage material. We hope this work can stimulate experimental research on TiN.

Acknowledgement

We thank our college management for their constant encouragement. The financial assistance from UGC, India is duly acknowledged with thanks.

References

- [1] A.Zerr, G.Miche, R.Riedel, *Nature matter.* 2 (2003) 185
- [2] J.C.Crowhurst, A.F. Goncharov, B. Sadigh, C.L. Evans, P.G. Morrall, J. L.ferreria, A.J. Nelson, *Science* 311 (2006) 1275.
- [3] V.A.Gasparov, N.S.Sidorov, I.I.Zverkova and M.P.Kulakov, *Pis'ma Zh. Eksp. Teor. Fiz.* 73, 604 (2001)
- [4] Liping ZHU, Masao Ohnishi and Shoji Yamanaka, *Material science and Engineering* (2009)
- [5] Dong CHEN, Jingdong CHEN), Yinglu ZHAO, Benhai YU, Chunlei WANG and Deheng SHI, *Acta Metall. Sin.(Engl. Lett.)* Vol.22 No.2 pp146-152 Apr. 2009
- [6] P.B. Allen, R.C. Dyenes, *Phys. Rev.* 12 (1975) 905.
- [7] H.L. Skriver, 'The LMTO method', Springer, Heidelberg (1984).
- [8] O.K. Anderson, *phys. Rev. B* 12, 3060 (1975).
- [9] O.K. Anderson and O. Jepsen, *phys. Rev. Lett.* 53, 2571 (1984)
- [10] O.K. Anderson, O. Jepsen and M. Sob, *Electronic band structure and its applications*, Editors. M. Yussouff, Springer Verlag Lecture Notes (1987).
- [11] F.D. Murnaghan, 'The Compressibility of Media under Extreme Pressures' in *Proceedings of the National Academy of Sciences*, vol. 30, pp. 244-247, 1944.
- [12] Francis Birch, 'Finite Elastic Strain of Cubic Crystals', in *Physical Review*, vol. 71, pp. 809-824 (1947).
- [13] M. Born, K. Huang, *Dynamical Theory of Crystal Lattices*, Clarendon, Oxford, 1956.

- [14] J.O. Kim, J.D. Achenbach, P.B. Mirkarimi, M. Shinn and S.A. Barnett, *J Appl Phys* 72 (1992) 1805.
- [15] C. Stampfl, W. Mannstadt, R. Asahi, and A. J. Freeman, *Phys. Rev. B* 63,155106 (2001).
- [16] R. Ahuja, O. Eriksson, J.M. Wills and B. Johansson, *Phys Rev B* 53 (1996) 3072.
- [17] J. C. Grossman, A. Mizel, M. Côté, M. L. Cohen, and S. G. Louie, *Phys.Rev. B* 60, 6343 (1999).
- [18] W. Wolf, R. Podloucky, T. Antretter, and F. D. Fisher, *Philos. Mag. B* 79,839 (1999).
- [19] H. Gou, L. Hou, J. Zhang, F. Gao, *Appl. Phys. Lett.* 92 (2008) 241901. [15] Y. Li, Zeng, *Chem. Phys. Lett.* 474 (2009) 93.
- [20] E. Sjöstedt, L.Nordström, D.J. Sing, *Solid state*
- [21] S.H. Jhi, J. Ihm, S. G. Louie, and M. L. Cohen, *Nature* 399,132 (1999).
- [22] E. I. Isaev I. Simak,I. A. Abrikosov R. Ahuja Yu. Kh. Vekilov M. I. Katsnelson A. I. Lichtenstein and B. Johansson, *JOURNAL OF APPLIED PHYSICS* 101, 123519 (2007)
- [23] W. Spengler, R. Kaiser, A. N. Christensen, and G. Müller-Vogt, *Phys. Rev.B* 17, 1095 -1978.
- [24] W. Weber, *Phys. Rev. B* 8, 5093 -1973.